

UNCLASSIFIED

AD 268 493

*Reproduced
by the*

**ARMED SERVICES TECHNICAL INFORMATION AGENCY
ARLINGTON HALL STATION
ARLINGTON 12, VIRGINIA**



UNCLASSIFIED

NOTICE: When government or other drawings, specifications or other data are used for any purpose other than in connection with a definitely related government procurement operation, the U. S. Government thereby incurs no responsibility, nor any obligation whatsoever; and the fact that the Government may have formulated, furnished, or in any way supplied the said drawings, specifications, or other data is not to be regarded by implication or otherwise as in any manner licensing the holder or any other person or corporation, or conveying any rights or permission to manufacture, use or sell any patented invention that may in any way be related thereto.

CATALOGED BY ASTIA

268493

AS AD 100

268 493

752850

INVESTIGATION OF CRYOGENIC GYRO

Contract No. NONR 474(09)

Prepared by:
R. E. Russell

Research Laboratories for the Engineering Sciences

University of Virginia

Charlottesville



62-1-5

XEROX

Report No. EE-4438-102-604

December 1961



SALE ANNOTATION AND SCHEDULE OF PRICES

| <u>No. of Pages</u> | <u>Price</u> |
|---------------------|--------------|
| 1 - 30 | .50 |
| 31 - 40 | .75 |
| 41 - 50 | 1.00 |
| 51 - 60 | 1.25 |
| 61 - 70 | 1.50 |
| 71 - 80 | 1.75 |
| 81 - 100 | 2.00 |
| 101 - 120 | 2.25 |
| 121 - 150 | 2.50 |
| 151 - 200 | 2.75 |

INVESTIGATION OF CRYOGENIC GYRO

Contract No. ~~N~~ONR 474(09)

Prepared by:
R. E. Russell

RESEARCH LABORATORIES FOR THE ENGINEERING SCIENCES
UNIVERSITY OF VIRGINIA
CHARLOTTESVILLE, VIRGINIA

Report No. EE-4438-102-61U

December 1961

Copy No. 9

TABLE OF CONTENTS

| | | |
|------------------------------|---|----|
| List of Illustrations | | 4 |
| SECTION I | INTRODUCTION | 5 |
| SECTION II | THE LONDON THEORY FOR A ROTATING SUPERCONDUCTOR | 8 |
| SECTION III | PRECESSION RATES DUE TO SPIN-INDUCED MOMENT | 12 |
| SECTION IV | INTERACTION OF THE SPIN-INDUCED MOMENT WITH THE SUPPORT FIELD GRADIENT | 19 |
| SECTION V | CONCLUSIONS | 26 |
| References | | 28 |

LIST OF ILLUSTRATIONS

| | | |
|----------|--|----|
| FIGURE 1 | Vectors Used to Describe Precession of the Spinning Superconducting Sphere | 15 |
| FIGURE 2 | Cryogenic Support Systems | 17 |
| FIGURE 3 | Hypothetical Support System Showing Image Coil Geometry | 21 |
| FIGURE 4 | Support Force for a Cryogenic Sphere | 23 |
| FIGURE 5 | Displacement of a Spring Cryogenic Sphere | 25 |

SECTION I INTRODUCTION

In order to meet the demand for improved inertial guidance systems, several new types of gyros have been proposed and are currently under development. Principal among these are the electrostatically and electromagnetically supported gyros and the cryogenic gyro.¹ Though differing widely in approach, each of these three types of gyro has one thing in common. The improvement in accuracy is achieved by freely suspending the gyro rotor in a nearly frictionless manner, reducing the external torques acting on the rotor to a small value.

The cryogenic gyro, employing a superconducting sphere, stably supported by a magnetic field, apparently would make an ideal gyro. Since the sphere would be in a perfectly superconducting state, the normal component of the support field could not enter the rotor, in accordance with the Meissner effect. Thus, all of the magnetic forces acting on the sphere would be normal to its surface, and there would be no error-producing torques.

In a practical case, certain undesirable torques do act on the rotor. These are due to pressure of the support field on blemishes in the rotor's surface, nonsphericity of the rotor, trapped flux, and mass unbalance. An order-of-magnitude estimation of these torques on the gyro performance was made in a report² by the Rand Corporation in 1957. This report concluded that, although an effective minimization of the torques was beyond the state of the art at that time, no fundamental difficulties with the basic principle of operation of a cryogenic gyro were apparent.

A number of research organizations then began experimental work on the cryogenic gyro. The program at General Electric has been described

¹ More esoteric types, such as the nuclear gyro have not yet reached the state of development of the three mentioned.

² W. H. Culver and M. H. Davis, "An Application of Superconductivity to Inertial Navigation," U. S. A. F. Project Rand Report R-363; January, 1957.

briefly by a number of press releases³ issued early in 1960.

General Electric had had difficulty in stably supporting a spinning sphere.⁴ Their support apparatus places the sphere within an outer housing, the clearance between the sphere and its housing being only 0.3 mm.⁵ When the sphere is rotated, it moves laterally with respect to the housing, eventually touching the wall. General Electric has attributed this loss of support to imperfections in the rotor.

In August of 1960, the Jet Propulsion Laboratory issued a technical release⁶ concerning its work on the cryogenic gyro. The report is a description of the work done to achieve a magnetic support system suitable for a cryogenic gyro. Although several successful support systems were described, no attempt was made to operate any of the supported spheres as a gyro. Subsequent to the issuing of the JPL report, a personal conversation⁷ disclosed that a solid niobium sphere had been successfully spun in a vacuum for a period of approximately 20 hours. If the rotating sphere had behaved as a gyro, its spin axis would have moved at earth rate with respect to the laboratory coordinates, returning to its original position at the end of 24 hours. However, the angular velocity of the rotor remained fixed in the laboratory system; e. g., aligned with the axis of the magnetic support coils. This failure of the spinning sphere to behave as a gyro was attributed to the presence of magnetic flux trapped in the rotor as it was cooled below the critical temperature. This source of torque could be eliminated by eliminating the trapped-in flux.

The London macroscopic theory of superconductivity describes a phenomenon which was investigated to determine if it could cause all or part of the difficulties experienced by JPL and GE. According to the London theory, a

³ See list of periodicals for press releases.

⁴ Private conversation with General Electric.

⁵ Chem. and Eng. News, February 1, 1960, 38:34.

⁶ Jet Propulsion Laboratory report, California Institute of Technology, Pasadena, California.

⁷ Personal conversation between Dr. Hardy (JPL) and Messrs. Harris and Denman (RLES).

rotating superconductor will have an induced magnetic dipole moment. This dipole moment is fixed in the same direction as the angular velocity of the rotating body, and is produced independently of any other magnetic fields which may be present. If the superconducting body is a magnetically supported sphere, the interaction of the rotationally induced moment with the support field will have two results: 1) the spin axis of the sphere will precess about or align with the support field; and 2) the spinning sphere will be displaced from its static position due to the interaction of the induced moment and the gradient of the support field.

The forces acting on the sphere due to the spin-induced magnetic moment cannot be eliminated by improvements in the state of the art. Therefore, it is important that an estimate of the effects of these forces on the performance of a cryogenic gyro be made. The calculations described in this report were made to determine the magnitude of these effects for configurations similar to the apparatus used by JPL and GE. Thus, the results of the numerical computations are applicable to existing experimental situations. The assumptions which were made to simplify the calculations did not alter the final results significantly.

The computations show that the effect of the spin-induced moment is too small to cause the difficulties encountered by JPL and GE. However, if the other sources of torque, e. g., trapped flux, are reduced to nominal levels, these effects would be observable. This offers the interesting possibility of validating London's rotating superconductor theory.

A section giving London's theory for a rotating superconducting sphere also is included in this report. The development is essentially that given by London, except that it has been reworked in rationalized MKS units used throughout this report. Although the treatment is by no means complete, it serves as a starting point for the applications which follow.

SECTION II
THE LONDON THEORY FOR A ROTATING SUPERCONDUCTOR

The material presented in this section follows closely the development given by London for the rotating superconductor.⁸ However, the equations in the London work, which were written in the Gaussian system of units have been rewritten here in the rationalized MKS system, used throughout this report.

In the rationalized MKS system, the London equations describing the state of a rotating superconductor are⁹

$$\nabla \Lambda \underline{v} = - \frac{e}{m_e} \underline{B} = - \frac{\mu_0 e}{m_e} \underline{H} \quad (1)$$

$$\dot{\underline{v}} = \frac{e}{m_e} \underline{E} \quad (2)$$

where \underline{v} is the velocity of the superconducting electrons and \underline{E} and \underline{H} are the electric and magnetic field vectors in the superconductor. A third relation may be obtained directly from Maxwell's equations,

$$\nabla \Lambda \underline{H} = n e (\underline{v} - \underline{v}_0) , \quad (3)$$

where \underline{v}_0 is the local state of motion of the superconducting body and n is the number of super-electrons in a unit volume. The displacement current is assumed to be zero.

If the superconducting body is a rotating sphere with an angular velocity, $\underline{\omega}$, and a radius r , then

$$\underline{v}_0 = \underline{\omega} \wedge \underline{r} .$$

⁸ F. London, Superfluids, vol. 1, p. 78, John Wiley and Sons, N. Y., N. Y. (1950).

⁹ m_e and e are the electronic mass and charge, respectively.

Also, in polar coordinates with ω directed along the polar axis,
 $\theta = 0,$

$$\begin{aligned}\nabla\Lambda\underline{v}_0 &= 2\underline{\omega} \\ \nabla\Lambda(\nabla\Lambda\underline{v}_0) &= 0 .\end{aligned}\tag{4}$$

Eliminating \underline{H} in equations (1) and (2) and using relation (4) gives

$$\nabla\Lambda [\nabla\Lambda(\underline{v} - \underline{v}_0)] = -\beta^2(\underline{v} - \underline{v}_0) ; \quad \beta^2 = \frac{\mu e^2 n}{m_e} .\tag{5}$$

This is the differential equation which must be solved to determine the velocities of the super-electrons within the superconducting sphere. The solution of this equation, in conjunction with equation (1), will determine the magnetic field within the sphere.

Outside the sphere, the differential equations of the field are just those for a vacuum,

$$\nabla \cdot \underline{B} = 0 , \quad \nabla\Lambda\underline{H} = 0 .$$

Taking into consideration the symmetry of the problem, the field outside of the body is assumed to be that of a dipole directed along the axis of rotation and at the center of the sphere ($r = 0$). The assumed solution is

$$\begin{aligned}H_r &= \frac{2m}{4\pi r^3} \cos \theta \\ H_\theta &= \frac{m}{4\pi r^3} \sin \theta && \text{for } r \geq R \\ H_\phi &= 0 .\end{aligned}\tag{6}$$

The constant, m , is the dipole moment of the field, and must be determined from the boundary conditions.

In the interior of the sphere, the solution for $(\underline{v} - \underline{v}_0)$ is assumed to

have only a ϕ component since \underline{v}_0 has only a ϕ component;

$$v_{0\phi} = \omega r \sin \theta .$$

Thus, the assumed solution is

$$v_{\phi} - v_{0\phi} = f(r) \sin \theta ,$$

or

$$v_{\phi} = [\omega r + f(r)] \sin \theta ,$$

where $f(r)$ is the radial dependence of the velocity field within the sphere. Substituting this into equation (5) gives the differential equation

$$f'' + \frac{2}{r} f' - \left(\frac{2}{r^2} + \beta^2 \right) f = 0 ,$$

the solution of which leads to the equation for v_{ϕ} ;

$$v_{\phi} = \left[\omega r + \frac{A}{r^2} (\sinh \beta r - \beta r \cosh \beta r) \right] \sin \theta , \quad r \leq R , \quad (7)$$

where A is a constant which must be determined from the boundary conditions.

The magnetic field within the sphere now can be determined by using equation (1) and the solution for v_{ϕ} . The components of the field are

$$H_r = \frac{m_e}{\mu_e} \left[2\omega + \frac{2A}{r^3} (\sinh \beta r - \beta r \cosh \beta r) \right] \cos \theta ;$$

$$H_{\theta} = \frac{m_e}{\mu_e} \left\{ -2\omega + \frac{A}{r^3} \left[(1 - \beta^2 r^2) \sinh \beta r - \beta r \cosh \beta r \right] \right\} \sin \theta \quad (8)$$

$$H_{\phi} = 0$$

for $r \leq R$. The boundary conditions require that the fields outside and inside

the sphere be equal at $r = R$. Equating (7) and (8) at $r = R$ gives two equations which can be solved for the constants A and m . Only the magnetic moment, m , is of particular interest. It is given by

$$m = \frac{4\pi m_e R^3}{\mu e} \omega \left[1 - \frac{3}{\beta R} \cosh \beta R + \frac{3}{\beta^2 R^2} \right] .$$

Since it was assumed that the dipole was oriented in the same direction as the angular velocity of the rotor, this equation can be written in vector form as

$$\underline{m} = \frac{4\pi m_e R^3}{\mu e} \underline{\omega} \left[1 - \frac{3}{\beta R} \coth \beta R + \frac{3}{\beta^2 R^2} \right] . \quad (9)$$

If the sphere has a radius much larger than $1/\beta$, and a relative permeability of one, equation (9) can be simplified to the relation

$$\underline{m} = \frac{m_e}{10^{-7} e} R^3 \underline{\omega} . \quad (10)$$

SECTION III
PRECESSION RATES DUE TO SPIN-INDUCED MOMENT

If a magnetic dipole is placed in a magnetic field, it will experience a torque acting to align the dipole with the field. The torque is given by

$$\underline{T} = \underline{m} \wedge \underline{B} \quad (11)$$

where \underline{B} is the magnetic field intensity and \underline{m} is the magnetic moment of the dipole. A magnetically supported superconducting sphere has a negative magnetic moment due to the surface supercurrents. This moment does not result in any torques on the sphere, the supercurrents being completely free to move within the sphere. However, the magnetic moment induced by the rotation of a superconducting sphere is fixed in the direction of the spin axis. Thus, there will be a torque acting to align the spin axis of the sphere with the support field. Depending upon the magnitude of the torque, the sphere will either precess about, or align with the field direction.

Suppose that we have a superconducting sphere, magnetically supported with the support field in the direction of the local vertical. Equation (11) can be written as

$$\frac{d\underline{L}}{dt} = \underline{m} \wedge \underline{B} \quad (12)$$

where

$$\underline{L} = I\omega$$

is the angular momentum of the sphere, with a moment of inertia, I . The value of \underline{m} was given in the previous section as

$$\underline{m} = \frac{m_e}{10^{-7}e} R^3 \underline{\omega} .$$

Substituting this, and for \underline{L} in equation (12), and solving for $\dot{\omega}$ gives

$$\dot{\underline{\omega}} = \frac{m_e}{10^{-7}e} \frac{R^3}{I} \underline{\omega} \wedge \underline{B} . \quad (13)$$

The vector \underline{B} can be rewritten as

$$\underline{B} = B \frac{\underline{b}}{|\underline{b}|}$$

where \underline{b} is a vector in the direction of the local vertical with a yet-undefined magnitude. Choosing

$$|\underline{b}| = b = \frac{m_e}{10^{-7}e} \frac{R^3}{I} B$$

gives equation (13) the simple form,

$$\dot{\underline{\omega}} = \underline{\omega} \wedge \underline{b} . \quad (14)$$

A similar expression can be derived for the motion of \underline{b} about the earth's axis,

$$\dot{\underline{b}} = \underline{k} \wedge \underline{b} , \quad (15)$$

where \underline{k} is parallel to the earth's axis of rotation with a magnitude equal to the angular velocity of the earth. A third equation is the obvious relation

$$\underline{k} = 0 . \quad (16)$$

It also is apparent that the magnitude of the vector $\underline{\omega}$ is a constant,

$$\frac{d}{dt} (\underline{\omega} \cdot \underline{\omega}) = 0 .$$

Since it then can be shown that

$$\frac{d}{dt} [\underline{\omega} \cdot (\underline{k} + \underline{b})] = 0 , \quad (17)$$

and that the magnitude of the vector $(\underline{k} + \underline{b})$ is also a constant, the angle between $\underline{\omega}$ and $(\underline{k} + \underline{b})$ must be constant. Therefore, the tip of the angular velocity vector describes a circle about the $(\underline{k} + \underline{b})$ vector in a plane perpendicular to the $(\underline{k} + \underline{b})$ vector as shown in Figure 1.

Using equations (14)-(16), the differential equations for the projection of $\underline{\omega}$ on two vectors orthogonal to $(\underline{k} + \underline{b})$, i. e., $(\underline{b} \wedge \underline{k})$ and $(\underline{k} + \underline{b}) \wedge (\underline{b} \wedge \underline{k})$ can be written

$$\frac{d^2}{dt^2} [\underline{\omega} \cdot (\underline{b} \wedge \underline{k})] = -\lambda^2 [\underline{\omega} \cdot (\underline{b} \wedge \underline{k})] \quad (18)$$

$$\frac{d^2}{dt^2} [\underline{\omega} \cdot (\underline{k} + \underline{b}) \wedge (\underline{b} \wedge \underline{k})] = -\lambda^2 [\underline{\omega} \cdot (\underline{k} + \underline{b}) \wedge (\underline{b} \wedge \underline{k})] , \quad (19)$$

where

$$\lambda^2 = |\underline{k} + \underline{b}|^2 .$$

The two vectors orthogonal to $(\underline{k} + \underline{b})$ are also shown in Figure 1.

It is apparent immediately from the form of the differential equations that their solution is harmonic in time. The entire solution for $\underline{\omega}$, from equations (17)-(19) is

$$\underline{\omega} = \omega \left\{ \frac{\underline{k} + \underline{b}}{|\underline{k} + \underline{b}|} \cos \delta + \sin \delta \left[\frac{\underline{b} \wedge \underline{k}}{|\underline{b} \wedge \underline{k}|} \cos \lambda t - \frac{(\underline{k} + \underline{b}) \wedge (\underline{b} \wedge \underline{k})}{|(\underline{k} + \underline{b}) \wedge (\underline{b} \wedge \underline{k})|} \sin \lambda t \right] \right\} \quad (20)$$

where δ is the angle between $\underline{\omega}$ and $(\underline{k} + \underline{b})$. Thus, the spin direction of the sphere precesses about the $(\underline{k} + \underline{b})$ vector with the angular frequency, λ ;

$$\lambda = |\underline{k} + \underline{b}| = (k^2 + b^2 + 2bk \cos \phi)^{1/2} \quad (21)$$

the angle ϕ being the co-latitude of the location of the experiment.

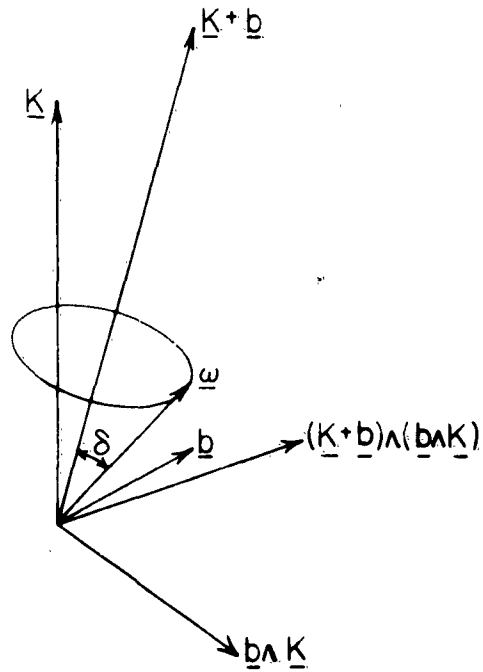


FIGURE I
 VECTORS USED TO DESCRIBE PRECESSION
 OF THE SPINNING SUPERCONDUCTING SPHERE

If the magnitude of \underline{b} were zero, the sphere would appear, in laboratory coordinates, to precess at earth rate, k_e , about the earth's polar axis. As b becomes large with respect to k_e , the sphere precesses about an axis almost parallel to \underline{b} , e. g., about the local vertical. In this instance, the sphere appears to be "locked in" with the support field.

Numerical values of b and λ were computed for a case similar to an experiment performed by JPL.¹⁰ The simplified configuration used for the computations is diagrammed in Figure 2a. A diagram of the actual configuration used by JPL is shown in Figure 2b. In order to simplify the computation of the magnetic field, the equatorial stabilizing coil used in the actual experiment was eliminated. The support position for a 1/2-inch diameter solid niobium sphere was found to be 7.5×10^{-3} meters with a coil mmf of 645 ampere turns. It was estimated from the JPL report describing the experiment that the support position was 6.40×10^{-3} meters with a support coil mmf of 1400 ampere turns. Since the field of the equatorial coil used in the JPL experiment opposes the support coil field¹¹, the total magnetic field strength is reduced. Thus, the computed position and total field strength for the simplified configuration are in close agreement with the estimates made from the JPL report.

The magnetic field along the axis of a circular loop of radius, a , is given in cylindrical coordinates by¹²

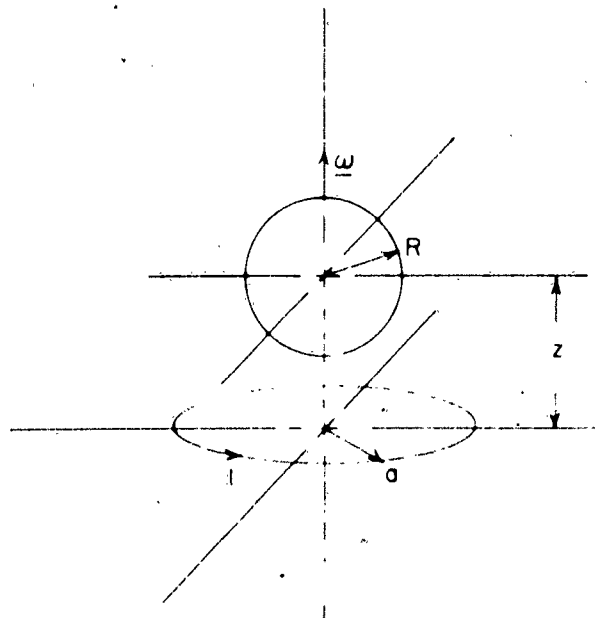
$$B_{\rho} = 0, \quad B_z = \frac{\frac{1}{2} \mu a^2 I}{(a^2 + z^2)^{3/2}}.$$

For the configurations of Figure 2a, the field at the point corresponding to the center of the supported sphere is 2.08×10^{-2} weber/m², giving for b a value of 2.09×10^{-6} radians/sec or 0.430 degrees/hr.

¹⁰ Technical Release No. 34-100, Jet Propulsion Laboratory, California Institute of Technology, Pasadena, California.

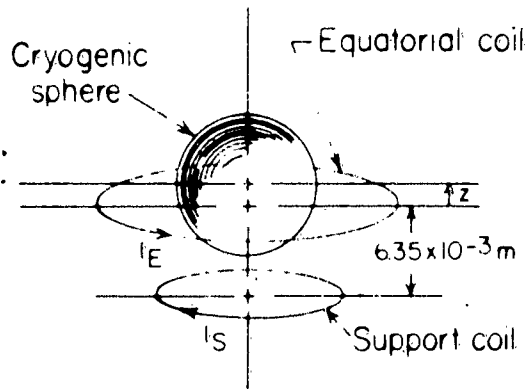
¹¹ The mmf of equatorial coil is usually about 1/3 of the support coil mmf.

¹² Smythe, "Static and Dynamic Electricity," p. 271, equation (8).



$R = 6.35 \times 10^{-3}$ METERS
 $a = 1.14 \times 10^{-2}$ METERS
 $I = 645$ AMPS
 $z = 75 \times 10^{-3}$ METERS

a. Simplified support configuration used to compute precession rate



b. Two coil support system

FIGURE 2
CRYOGENIC SUPPORT SYSTEMS

Using this value for b in equation (21) gives a precession rate, λ , of 15.3 degrees/hr. Earth rate, k , is 15 degrees per hour and the colatitude, ϕ , for Pasadena, California, the location of JPL, is 52 degrees north.

The motion of the sphere can be described as follows: The spin vector of the sphere will precess about a vector ($\underline{k} + \underline{b}$) at a rate of 15.3 degrees per hour. If there were no torque acting on the sphere, it would precess uniformly about a direction parallel to \underline{k} and at a rate of 15 degrees/hour.

SECTION IV
 INTERACTION OF THE SPIN-INDUCED MOMENT WITH THE
 SUPPORT FIELD GRADIENT

There are three forces acting on a spinning, perfectly superconducting sphere supported by a magnetic field. Two of these forces are the support force, and the inertial reaction due to a linear acceleration of the rotor. A third force is the result of the interaction of the gradient of the support field with the magnetic moment induced by the rotation of the sphere. This force is given by

$$\underline{F} = (\underline{m} \cdot \nabla) \underline{B}$$

where \underline{m} is the induced magnetic moment and \underline{B} is the magnetic support field flux density. Using the equation for the induced moment derived in Section II,

$$\underline{m} = \frac{m_e}{10^{-7}e} R^3 \underline{\omega} ,$$

the force becomes

$$\underline{F}(\underline{\omega}, \underline{r}) = \frac{m_e}{10^{-7}e} R^3 (\underline{\omega} \cdot \nabla) \underline{B}(\underline{r}) . \quad (22)$$

Here, the vector \underline{r} is the position of the center of the sphere with respect to the chosen origin. Thus, the force equation for the supported sphere is

$$\underline{F}(\underline{r}) + \underline{F}(\underline{\omega}, \underline{r}) + m\underline{a} = 0 \quad (23)$$

where $\underline{F}(\underline{r})$ is the support force and $m\underline{a}$ is the inertial reaction.

Equations (22) and (23) can be simplified greatly if some assumptions are made about the gyro configuration. Assuming that the support field is cylindrically symmetric with a component, B_z , in the direction of the local vertical and, further, that the spin axis of the sphere also is directed along the same vertical, equation (22) reduces to

$$F(\omega_z, z) \frac{m_e}{10^{-7}e} R^3 \omega_z \frac{\partial B_z}{\partial z} . \quad (24)$$

Also, if there are no accelerations acting on the sphere except the acceleration of gravity, there is only a vertical component of the support force. Equation (23) then becomes

$$F(z) + F(\omega, z) - mg = 0, \quad (25)$$

which can be solved to determine the position of the rotor as a function of its angular velocity.

If the support magnetic field is produced by a circular loop, the support force $F(z)$ is computed readily for a spherical rotor by using an image method. Figure 3 shows a hypothetical support system using two circular loops with opposing fields. This configuration is similar to the type of support used by General Electric in their experimental gyro. The geometry for the image coil also is illustrated for the lower coil. To determine the force on the sphere, the size, current, and location of the image coil is determined first. This computation needs to be made for only one of the two loops since the solution can be modified easily by a change of coordinates to provide the force between the second loop and the sphere. The total force is found by adding the two solutions.

Smythe¹³ gives the equation for the force between two circular loops as

$$f = \frac{\mu_0 I_1 I_2 \zeta}{[(a + \omega)^2 + \zeta^2]^{1/2}} \left[-K + \frac{(a^2 + b^2 + \zeta^2)E}{(a - b)^2 + \zeta^2} \right], \quad (26)$$

where K and E are the elliptic integrals of the first and second kinds, respectively, with the modulus k given by

$$k^2 = \frac{4ab}{(a + b)^2 + \zeta^2}.$$

The image variables, I_1 , ζ , and b are given in terms of the coordinate z , by

¹³ Smythe, op. cit., p. 281, equation (2).

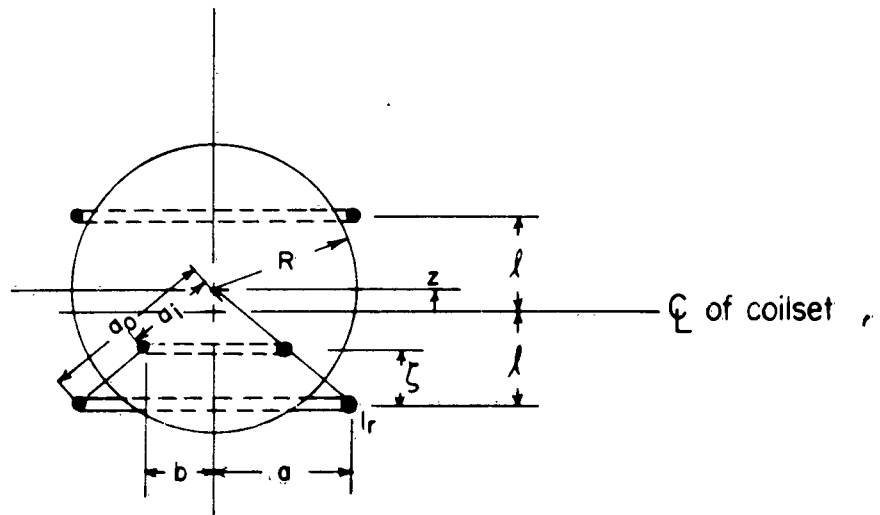


FIGURE 3
 HYPOTHETICAL SUPPORT SYSTEM
 SHOWING IMAGE COIL GEOMETRY

$$b = \frac{aR^2}{a^2 + z^2}, \quad \zeta = z\left(1 - \frac{R^2}{a^2 + z^2}\right), \quad I_i = \frac{(a^2 + z^2)^{1/2}}{R} I.$$

These relations are derived easily from the well-known relations between the image and real loops for a sphere,

$$a_i = \frac{R^2}{a_o}, \quad I_i = \frac{a_o}{R} I_r,$$

and the system geometry.

Numerical values of $F(z) - mg$, computed for a 4-cm diameter niobium sphere, such as is used by GE, are plotted in Figure 4. The other constants necessary for computing the force were chosen to be

$$a = 1.9 \times 10^{-2} \text{m}$$

$$\ell = 1.02 \times 10^{-3} \text{m}$$

$$I = 633 \text{ amperes/coil}.$$

The support coil current was fixed by restricting the maximum magnetic field at the rotor surface to be less than the critical field strength of niobium. Thus, a current of 633 amperes in the coils produces a field strength of 0.15 weber/m² at the rotor surface. The critical field strength of niobium is 0.2 weber/m² at 4.2°K.

Now, solving equation (25) for ω_z gives

$$\omega_z = (mg - F_z) \left(\frac{\partial B}{\partial z}\right)^{-1} \left(\frac{10^{-7} e}{m_e R^3}\right). \quad (27)$$

The magnetic field gradient, $\partial B_z / \partial z$, is found easily from the equation for the field along the axis of a circular loop, as given by Smythe.¹²

For two loops located at distances $\pm \ell$ from the origin, as in Figure 3, the gradient is

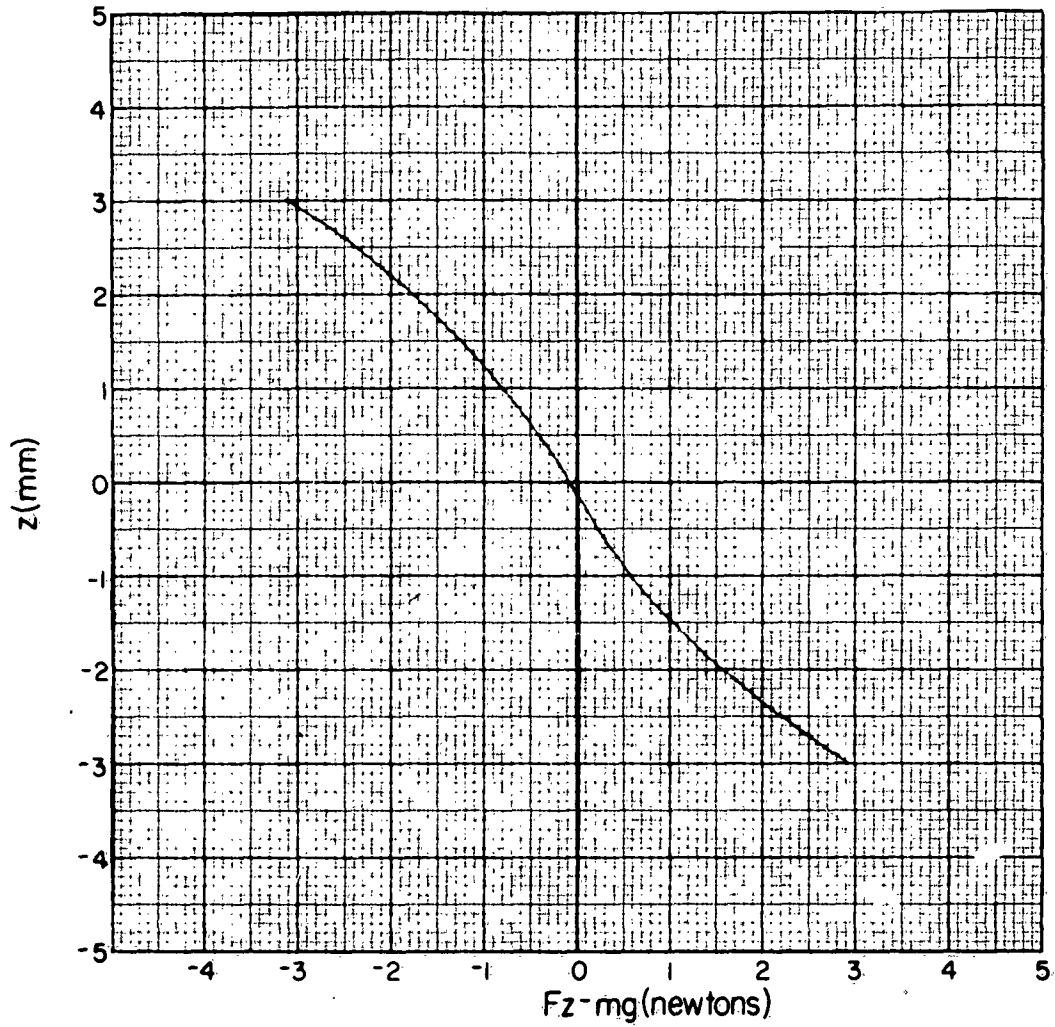


FIGURE 4
SUPPORT FORCE FOR A CRYOGENIC SPHERE

$$\frac{\partial B}{\partial z} = \frac{3}{2} \mu a^2 I \left\{ \frac{l - z}{[a^2 + (l - z)^2]^{3/2}} + \frac{l + z}{[a^2 + (l + z)^2]^{3/2}} \right\} .$$

Figure 5 is a plot of the solution of equation (27) for values of z ranging from $+3 \times 10^{-3}$ meters to -3×10^{-3} meters. However, the ordinate and abscissa reversed so that the graph shows the position of the sphere as a function of its angular velocity. The slope of the line is -1.25×10^{-12} meters/radian/sec. Thus, an extremely high rotational speed would be required to cause a significant change in sphere position.

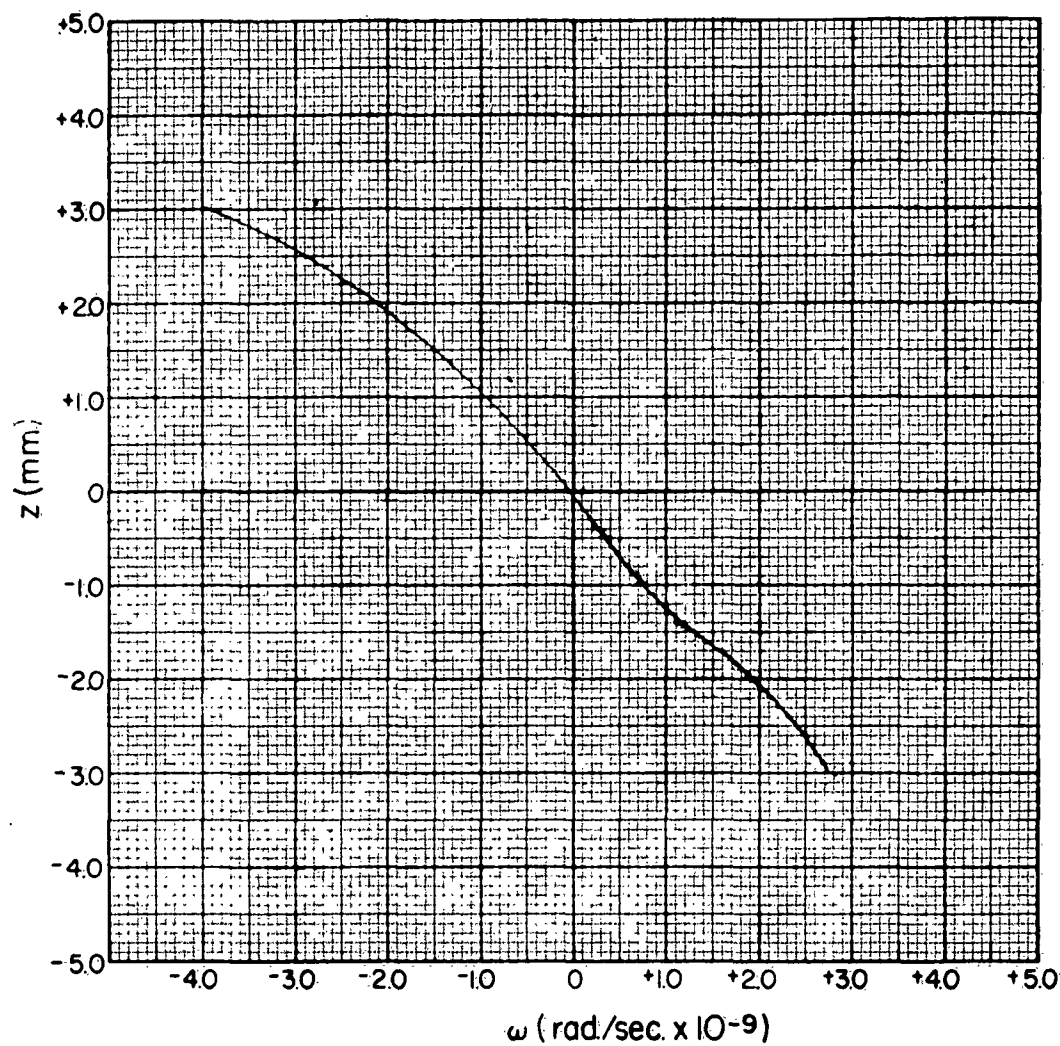


FIGURE 5
DISPLACEMENT OF A SPINNING CRYOGENIC SPHERE

SECTION V CONCLUSIONS

The computations in this report were made to determine the extent to which the presence of a rotationally induced magnetic moment would affect a cryogenic gyro. Specifically, two cases similar to experiments performed by JPL and GE were considered. The difficulties experienced by the JPL and GE experimenters could have been the result of the interaction of the induced moment with the support field.

As stated in Section III, the magnitude of \underline{h} must be large compared to the magnitude of \underline{k} if the angular velocity of the sphere is to "lock in" with the magnetic field. This criteria is not fulfilled for the case similar to the JPL experiment, the magnitude of \underline{h} being only 0.430 degrees/hr., as compared to 15 degrees/hr. for the magnitude of \underline{k} . Therefore, the "lock in" observed at JPL was indeed most probably due to flux trapped in the rotor.

However, it is interesting to note that the precession rate due to the spin-induced moment is large enough to affect the gyro performance. Also, this precession rate is independent of the angular velocity of the rotor and cannot be reduced by increasing the spin rate of the sphere. One method for reducing the drift is to increase the moment of inertia of the sphere, particularly in a manner which would give a preferred spin axis. Another method is to servo the support field so that it is always parallel to the spin axis of the rotor. Since the torque which causes the precession of the sphere is proportional to the sine of the angle between the field and spin axis, the drift rate is reduced by keeping this angle small.

Finally, this torque is absent if the rotor is supported in the center of a symmetrical magnetic field, such as is used by GE. However, the rotor will move from the zero field position if the gyro undergoes an acceleration. It then will begin to precess.

As can be seen in Figure 5 (Section IV), an angular velocity of about 8×10^7 radians/sec is required to cause the rotor to move a distance of 0.3

mm. the clearance in the GE gyro configuration. This is a rotor speed of 1.3×10^6 rps. This speed is obtainable only with very small rotors and is much faster than the speed of operating gyros. Therefore, it can be concluded that the effect is not large enough to cause the loss of support as found by GE. The small motion probably can be neglected in most gyroscope applications.

One or both of the two effects, precession or displacement of a spinning cryogenic sphere, might be used to demonstrate the validity of the London theory. The precession rate of a spinning sphere is certainly large enough to be easily observable, but is easily masked by other sources of torque such as trapped flux. Most of the same problems which affect the cryogenic gyro would have to be solved before this type of experiment would be possible. The other effect, the displacement of a spinning rotor, is extremely small for the sphere size chosen for the computations in this report. However, reducing the rotor size increases the rotor speeds that can be obtained, and such an experiment may become practical. No computation of the speed-displacement characteristic of a small rotor have been made yet. Such a computation should be made to determine the practicability of performing this type of experiment.

REFERENCES

(List of Periodical References Concerning General Electric's Gyro)

Chemical and Engineering News, 38:34, February 1, 1960.

Control Engineering, 7:38, March 1960.

Electrical Engineering, 79:344, April 1960.

Machine Design, 32:14-15, February 4, 1960.

Mechanical Engineering, 82:78-79, March 1960.

DISTRIBUTION LIST

Copy No.

1 - 10 Director
 Armed Services Technical Information Agency
 Arlington Hall Station
 Arlington, Virginia

11 - 12 Chief of Naval Research
 Code 466
 Washington 25, D. C.

13 - 15 Director
 U. S. Naval Research Laboratory
 Washington 25, D. C.
 ATTN: Code 2027

16 Director
 U. S. Naval Research Laboratory
 Washington 25, D. C.
 ATTN: Code 5362

17 Director
 Special Projects Office
 SP-24
 Navy Department
 Washington 25, D. C.

18 Chief, Bureau of Ships
 Code 665 H
 Washington 25, D. C.

19 Dr. F. J. Weyl
 Office of Naval Research
 Washington 25, D. C.

20 Dr. W. H. Avery
 Applied Physics Laboratory
 The Johns Hopkins University
 8621 Georgia Avenue
 Silver Spring, Maryland

21 Chief of Naval Operations (OP07T2G)
 Department of the Navy
 Washington 25, D. C.

- 22 Dr. D. F. Bleil
Naval Ordnance Laboratory, White Oak
Silver Spring, Maryland
- 23 Dr. R. J. Christensen
U. S. Naval Electronics Laboratory
San Diego 52, California
- 24 Captain W. H. Cross
Bureau of Ships (Code 403)
Department of the Navy
Washington 25, D. C.
- 25 Dr. P. M. Fye
Woods Hole Oceanographic Institute
Woods Hole, Massachusetts
- 26 Dr. E. S. Lamar
Bureau of Naval Weapons (CR-12)
Department of the Navy
Washington 25, D. C.
- 27 Dr. T. Phipps
U. S. Naval Ordnance Test Station
China Lake, California
- 28 Captain W. T. Sawyer
Office of Naval Research (Code 406)
Washington 25, D. C.
- 29 Dr. George Sponsler
Bureau of Ships
Department of the Navy
Washington 25, D. C.
- 30 Dr. W. F. Whitmore
Missile and Space Division
Lockheed Aircraft Corporation
Palo Alto, California
- 31 LCDR R. H. Yerbury (Executive Secretary)
Special Projects Office (SP-114)
Bureau of Naval Weapons
Washington 25, D. C.
- 32 A. R. Kuhlthau
- 33 E. C. Stevenson
- 34 O. R. Harris

| | |
|---------|------------------|
| 35 | B. J. Gilpin |
| 36 | R. E. Russell |
| 37 | L. R. Quarles |
| 38 | Reports Section |
| 39 - 40 | Alderman Library |
| 41 - 50 | RLES Files |